

# Positive Contrast and Quantitative Imaging of Magnetic Nanoparticles and Cancer Cells with Biomarker Targeted RGD-Nanoparticle Conjugates Using T<sub>1</sub> Weighted Ultrashort Echo Time (UTE) Imaging

X. Zhong<sup>1</sup>, L. Zhang<sup>2,3</sup>, L. Wang<sup>2</sup>, H. Chen<sup>2</sup>, J. Yeh<sup>2</sup>, A. Wang<sup>4</sup>, and H. Mao<sup>2</sup>

<sup>1</sup>MR R&D Collaborations, Siemens Healthcare, Atlanta, GA, United States, <sup>2</sup>Department of Radiology, Center for Systems Imaging, Emory University, Atlanta, GA, United States, <sup>3</sup>Department of Radiology, Jinling Hospital, Nanjing University College of Clinical Medicine, Nanjing, Jiangsu, China, People's Republic of, <sup>4</sup>Ocean NanoTech, LLC, Springdale, AR, United States

**Introduction.** Magnetic nanoparticles (MNPs) have been introduced as contrast agents for magnetic resonance imaging (MRI) and molecular imaging probes because of their superb ability in shortening T<sub>2</sub> and T<sub>2</sub>\* of the tissue, leading to a strong decrease in signal intensity of target organs or “negative” contrast on T<sub>2</sub> weighted images (1,2). However, the typical drawback of the negative contrast is its poor contrast to noise ratio (CNR) when used to study areas that have low background signals, such as liver or spleen. Furthermore, benefit of using large sized MNPs that offer high magnetic susceptibility and strong T<sub>2</sub> effect may not be realized by negative contrast, as CNR may not improve further beyond voiding the signal from its original level. This work reports that signal enhancing or positive contrast of MNPs and MNP-bounded cancer cells can be obtained using ultrashort echo time (UTE) MRI with quantitative correlations between the positive contrast and the size and concentration of MNPs.

Table 1 Core sizes and concentrations of IONP samples. The R<sub>1</sub> and R<sub>2</sub> values that are not measurable by the experiment settings in this study are marked as NA.

Core size (nm)	Concentration (mol/l) / R <sub>1</sub> (s <sup>-1</sup> ) / R <sub>2</sub> (s <sup>-1</sup> )				
4.8	0.024 / 0.3765 / 1.1017	0.119 / 0.4794 / 1.6892	0.239 / 0.6667 / 2.2356	0.478 / 0.7013 / 2.9240	0.956 / NA / NA
8.7	0.026 / 0.8621 / 10.3199	0.129 / 1.5723 / 37.0370	0.258 / 2.4691 / 59.8802	0.516 / 5.4645 / 96.1538	1.032 / NA / NA
13.4	0.020 / 0.8389 / 15.3846	0.100 / 1.5337 / 53.4759	0.201 / 2.2173 / 88.4956	0.401 / 6.2893 / 147.0588	0.803 / NA / NA
25.4	0.022 / 0.6789 / 16.3934	0.112 / 1.7422 / 52.9101	0.225 / 3.5587 / 84.0336	0.449 / 7.6923 / 156.2500	0.898 / NA / NA

**Methods.** All MRI experiments were performed on a 3 T scanner (Siemens, Magnetom Tim Trio). Iron oxide nanoparticles (IONPs) with four different core sizes were prepared and coated with amphiphilic triblock copolymers as previously reported (3). The averaged size of each IONP was accurately measured from electron microscopy image. Five different concentrations of IONPs colloidal solutions at each size were prepared with concentrations determined by chemical analysis. T<sub>1</sub> values of the samples were measured using an inversion recovery spin echo (SE) sequence with TE of 8.5 ms and TR of 1500ms at different TI of 23, 46, 92, 184, 368, 650, 850, 1100 and 1400 ms, respectively. T<sub>2</sub> values were measured using a multi-echo SE sequence with TR of 2000 ms and 20 TEs starting at 10 ms with increment of 10 ms. T<sub>1</sub> and T<sub>2</sub> values were calculated using non-linear curve fitting based on the Levenberg-Marquardt algorithm and using non-linear exponential curve fitting, respectively. A multi-echo UTE sequence described previously (4) was used for imaging all IONP samples. This sequence consists of one 60 μs non-selective RF pulse followed by a 40 μs transmit/receive switch time, and a 100% asymmetric data acquisition from the center to the surface of a sphere in the k-space using a 3D radial sampling trajectory. The shortest TE used for this study was 0.07 ms; the second and longer TE was 2.76 ms. Other parameters included TR = 21.7 ms, flip angle = 15°, FOV = 22 × 22 cm<sup>2</sup>, image matrix = 192 × 192, bandwidth = 64000 Hz/pixel, total radial projections = 40000, radial projections per excitation = 176, averages = 2. For comparison, conventional T<sub>2</sub> weighted SE imaging were also performed with parameters including TR = 1000 ms, TE = 9.3 ms, image matrix = 320 × 320, slice thickness = 4.0 mm, FOV = 22 × 22 cm<sup>2</sup>. To quantify the contrast enhancing effect of UTE and conventional T<sub>2</sub> weighted methods in imaging of IONP samples, a simple CNR analysis was performed as  $CNR = |I_{IONP} - I_{water}| / I_{water}$ , where I<sub>IONP</sub> and I<sub>water</sub> are the signal intensity of the IONP sample and the pure water, respectively.

Human glioma U87 cells were cultured and then incubated in serum-free RPMI media with a 0.1 mM concentration of tri-peptide RGD conjugated IONP (10 nm, core size), targeting α<sub>v</sub>β<sub>3</sub> integrin overexpressed in U87 cells, for two hours at room temperature. Binding of RGD-IONP to U87 cells was confirmed using Prussian blue staining cell samples for iron. RGD-IONP bound cells were washed with PBS and then scraped from the flasks. Collected cells were re-suspended non-uniformly in 1 ml of 2% agarose gel containing different numbers of cells for MRI.

**Results.** The core size, concentration, R<sub>1</sub> and R<sub>2</sub> values of the IONP samples are listed in Table 1, where some of R<sub>1</sub> and R<sub>2</sub> values are not measurable due to the signal voids of high concentration. Linear correlations are observed between the available R<sub>1</sub> and R<sub>2</sub> values and the core size or the concentration (data not shown). Although both the R<sub>1</sub> and R<sub>2</sub> values increase as the core size or the concentration of IONPs increases, the increment level of R<sub>2</sub> is much stronger than that of R<sub>1</sub>, i.e. the T<sub>2</sub> effect is more dominant than the T<sub>1</sub> effect. This is evident in the conventional T<sub>2</sub> weighted SE images, where the signal intensity decreases and voids with the increased core size or concentration (Fig 1a). In contrast, since the T<sub>2</sub> effect in UTE imaging can be usually neglected due to the very small TE, UTE images are T<sub>1</sub> weighted and exhibit signal enhancement with the increased core size or concentration (Fig 1b). The signal enhancement of UTE images over the range of core size and concentration of IONPs in this study are plotted in Fig 2a and 2b, respectively. Except the IONP with the core size of 4.8 nm, the CNR of UTE images are 3 to 4 times higher than that of T<sub>2</sub> weighted images (data not shown). UTE imaging of RGD-IONP bound U87 glioma cells exhibited positive contrast enhancement comparing to signal drops in T<sub>2</sub> weighted imaging (Fig 3). The higher number of RGD-IONPs bound cells, the higher signal intensity in UTE imaging was observed.

**Conclusion.** This study demonstrated that positive T<sub>1</sub> contrast from IONPs can be obtained using UTE imaging, resulting higher CNR compared to that of conventional T<sub>2</sub> weighted imaging. Signal intensity of IONPs in UTE images has a linear correlation with core size and concentration of IONPs in the ranges used in this study. Cell imaging with the UTE method also demonstrated potential applications of UTE imaging of biomarker targeted IONPs with contrast enhancement associated to the binding of cell targeted MNP.

**Acknowledgement.** This work is supported in parts by NIH grants of U54CA119338 and P50CA128301, and a grant from EmTech Bio.

1. Chambon et al. Magn Reson Imaging 1993;11:509-519.
2. Simon et al. Eur Radiol 2006;16:738-745.
3. Duan et al. J Phys Chem C 2008 ;112(22) :8127-8131.
4. NIELLES-VALLESPIN et al. 17th ISMRM 2009;2654.

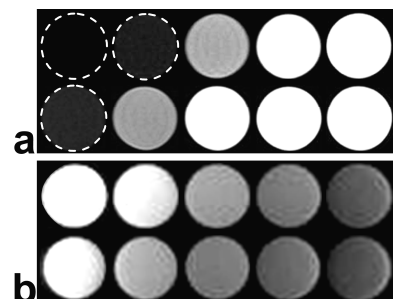


Fig. 1 (a) Conventional T<sub>2</sub> weighted SE images of IONP samples, where the top and bottom samples have core size of 25.4 nm and 8.7 nm, respectively, and the concentrations decrease from left to right. (b) UTE T<sub>1</sub> weighted images of the same samples.

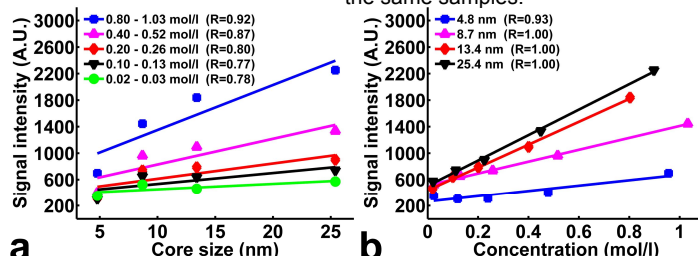


Fig. 2 Plots of signal intensity of UTE T<sub>1</sub> weighted images vs (a) core size and (b) concentration of IONP samples.

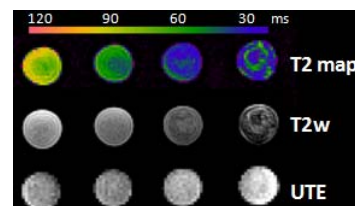


Fig. 3 Comparison of T<sub>2</sub> maps, T<sub>2</sub> weighted SE images and UTE T<sub>1</sub> weighted images of cell phantoms containing 1, 2, 3 and 4x10<sup>6</sup> RGD-IONP bound U87 cells.